Three-Dimensional Base Distributed Effects of Long Stripe BJT's: Base Resistance at DC

Ming-Yeh Chuang, Mark E. Law, *Senior Member, IEEE*, and Kenneth O, *Member, IEEE*

Abstract— An analytical model describing the dc voltage and current distributed effects in the polysilicon and intrinsic base regions of long stripe BJT's with double polysilicon technology is presented. It is shown that the bias dependent debiasing effect in the base polysilicon contacts causes an unequal division of base current between two base polysilicon contacts and results in a re-distribution of base current in the base regions at different levels of current injection. The base resistance is also modulated by this current re-distribution effect at different biases. The change of base resistance with bias is calculated and the results show the importance of the distributed effects in the base polysilicon region in determining the base resistance.

Index Terms— Base resistance, bipolar transistor, debiasing, device simulation, three-dimensional.

I. INTRODUCTION

BASE resistance is important for characterizing the large- and small-signal behavior [1], switching characteristics [2], [3] and noise performance [4], [5] of high-speed bipolar transistors. The accurate determination of the base resistance is essential for BJT design and modeling. It is known that the base resistance decreases as the operating current increases due to base conductivity modulation, base push-out in high-level injection, and current crowding effects [6]–[8]. The crowding is the tendency for current to flow at the edge of the intrinsic base region at high-level current injection due to a voltage drop along the base current path in the intrinsic base region. The current crowding reduces the effective base current path and decreases the base resistance. Accurate modeling of base resistance is complicated due to its distributed nature and operating point dependence.

Several papers have discussed modeling and computation of the base resistance based on the debiasing and current crowding effect in the two-dimensional (2-D) intrinsic base region of BJT's [6], [9]–[12] with the assumption that the voltage and current distribution in the third dimension are uniform. Schroter [13] proposed a purely geometry-dependent model to compute the external base resistance. However, in contemporary high-speed double polysilicon BJT's, a long stripe (see Fig. 1) or long interdigitated base structure is often used to obtain high current drive and low base resistance. In this situation, similar debiasing effect occurs in the polysilicon region as in the intrinsic base region which causes nonuniform voltage and current distribution in the third dimension of the device. The voltage and current distribution characteristics
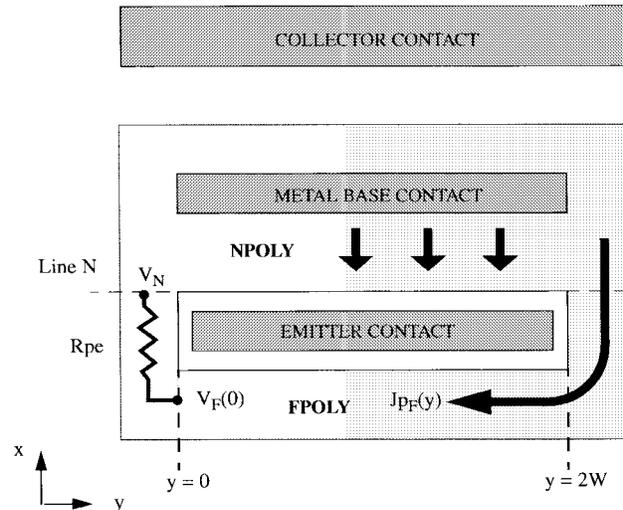
Fig. 1. Top view of a long stripe BJT with single metal, double polysilicon base contact structure used in this work. The arrow signs indicate the low and high resistive current paths for NPOLY and FPOLY, respectively.

vary at different base-emitter biases resulting in the modulation of base resistance. To date, the debiasing effect in the base polysilicon region and the three-dimensional (2-D) nonuniform current distribution in the base along with its relationship to the base resistance at different biases has not been studied.

In Section II, a quasi-2-D base voltage and current distributed model of long stripe BJT's are derived. In Section III, the 2-D distributed bias effects in the active as well as polysilicon base regions are demonstrated, and the resultant nonuniform current distribution will be presented as a function of dc bias. Finally, in Section IV, the effective base resistance at different dc biases are calculated and compared with measured data and results from a 2-D model. Using the results, effects of scaling and silicide technologies on the base resistance and device design consideration are also examined.

II. MODEL DEVELOPMENT

Fig. 1 shows a typical stripe BJT with single metal, double polysilicon base contact structure which will be used to study the 2-D voltage and current distributed effect. The base current in the polysilicon region can be divided into two major components. One flows from the metal base contact and injects directly into the intrinsic base region at NPOLY (Near POLY) side. The other component flows through FPOLY (Far POLY) before it is injected into intrinsic base region. Although the base current density flowing from metal contact to the edge of NPOLY (lineN in Fig. 1) might be different, the voltage along lineN can be assumed to be constant $(= V_N)$ due to the
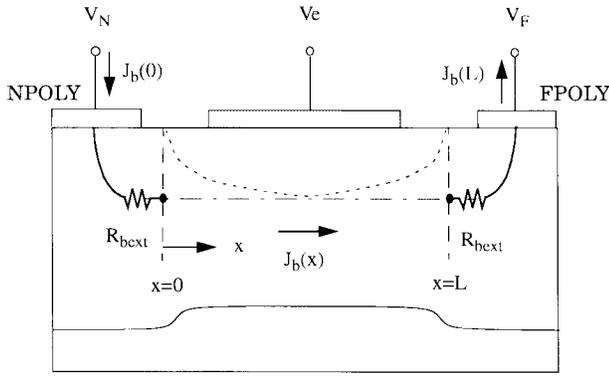
- - - - -   Path to extract potential in device simulation

- - - - - - -   Base-emitter metallurgical junction in the device

Fig. 2.   Schematic diagram of the active region in the BJT. Shaded regions are the polysilicon emitter and base contacts. A lumped extrinsic base resistance $R_{b\text{ext}}$ connects the base polysilicon contact and intrinsic base region. All the base current injected into the intrinsic base area flows through $R_{b\text{ext}}$.

small resistance and negligible ohmic voltage drop difference in the short and wide current path. The base current flowing through FPOLY experiences larger resistance due to a longer and narrower current path compared with current in NPOLY, which results in a larger debiasing effect in FPOLY. The voltage varies along FPOLY and is expected to be lower than that of NPOLY.

To simplify the problem, we assume the base current injects from base polysilicon contact to the intrinsic base region boundary through a lumped extrinsic base resistance $R_{b\text{ext}}$ without any current loss (see Fig. 2). The base current in the intrinsic base region is also assumed to flow only in the x-direction and has no current component in the y-direction. If the stripe is long, the base current contributed from the short edges of the emitter is negligible. The base current in FPOLY can then be assumed to flow only in y-direction and conduct from NPOLY through a lumped resistance Rpe at the edges of polysilicon base handle as shown in Fig. 1. Thus, the device can be treated as the integration of numerous slices of 2-D structures in the y-direction.

Based on the assumptions and derivations of Hauser [14], the base current $J_b(x)$ and voltage $V(x)$ in the 2-D intrinsic base region (see Fig. 2) are given, respectively, by

$$J_b(x) = \frac{2V_{\text{TH}}}{\rho_b} \cdot Z \cdot \tan(Z \cdot (l - x)) \tag{1}$$

and

$$V(x) = V(0) - 2V_{\text{TH}} \ln\left(\frac{\cos(Z \cdot (l - x))}{\cos(Zl)}\right) \tag{2}$$

where ρ_b is the intrinsic base resistivity, l is the minimum voltage point in intrinsic base region, $Z_{\text{TH}} = KT/q$ is the thermal voltage, Z can be obtained from the solution of the equation

$$\left(Z \frac{L}{2}\right) \cdot \tan\left(Z \frac{L}{2}\right) = \frac{\rho_b L}{4V_{\text{TH}}} \cdot J_b(0) \tag{3}$$

and L is the intrinsic base length. Hauser assumed the biases at both sides of the intrinsic base are the same and obtained $l = L/2$. For asymmetric base biases, l can be obtained by solving (2) and is given by

$$l = \frac{1}{Z} \cdot \operatorname{atan}\left(\frac{1}{\sin(ZL)} \cdot \exp\left(\frac{V(0) - V(L)}{2V_{\text{TH}}}\right)\right.$$
$$\left. - \cot(ZL)\right). \tag{4}$$

Combining (1) and (2), and assuming $|V(0) - V(L)| \ll 2V_{\text{TH}}$ to linearize the equations, the J-V relation in the intrinsic base boundary is given by

$$J_b(0) = \left(\frac{Z}{\rho_b \sin(ZL)}\right)(V(0) - V(L))$$
$$+ \frac{2V_{\text{TH}}Z}{\rho_b} \tan\left(\frac{ZL}{2}\right) \tag{5a}$$

and

$$J_b(L) = -\left(\left(\frac{Z}{\rho_b \sin(ZL)}\right)(V(L) - V(0))\right.$$
$$\left. + \frac{2V_{\text{TH}}Z}{\rho_b} \tan\left(\frac{ZL}{2}\right)\right). \tag{5b}$$

If the lumped extrinsic base resistance $R_{b\text{ext}}$ is taken into account, the relation between the terminal current density in the base polysilicon contacts and voltage $V_F(y)$ in FPOLY is then given by

$$J_{bN}(y) = J_b(0) = C_1 \cdot V_F(y) + C_2 \tag{6a}$$
$$J_{bF}(y) = -J_b(L) = -C_1 \cdot V_F(y) + C_3 \tag{6b}$$

where (see (7)–(9) shown at the bottom of the next page) and $J_{bN}(y)$ and $J_{bF}(y)$ are the base currents injecting from NPOLY and FPOLY, respectively. If ρ_b and $R_{b\text{ext}}$ are independent of the current crowding effect at each bias V_N, and the total base current J_{bt} is constant, then C_1, C_2, and C_3 become constants. Thus, the base current densities injected from NPOLY $Jb_N(y)$ and FPOLY $Jb_F(y)$ into the active base region are linear functions of $V_F(y)$, which is determined by the debiasing effect along FPOLY.

The following assumptions have been made while deriving the expressions for current and voltage distribution in the polysilicon base regions: 1) the resistivity of polysilicon base ρ_p is constant, 2) the current density in FPOLY is uniformly distributed in the direction perpendicular to the current flow (y-direction), and 3) the device is symmetric in y-direction. Using the same methodology as used in deriving current and voltage in the intrinsic base region, the transverse base current density $Jp_F(y)$ in FPOLY with a cross section area of A_p can be expressed as

$$Jp_F(y) = C_5 \cdot \sinh(C_4 \cdot (y - W)) \tag{10}$$

where

$$C_4 = \sqrt{\left(-\frac{C_1 \cdot \rho_p}{Ap}\right)} \tag{11}$$

$$C_5 = -\frac{Jp_F(0)}{\sinh(C_4 W)} \tag{12}$$

and W is half of the emitter stripe length. The voltage $V_F(y)$

TABLE I
THE DEVICE PARAMETERS REQUIRED FOR MODEL

parameters	value
Emitter width (Intrinsic base length), L	1μm
Intrinsic base width, W_b @Vbe=0.6V, Vcb=2V	0.22μm
Unit length extrinsic base resistance, R_{bext}	705.3Ω·μm
Intrinsic base resistivity, ρ_b @Vbe=0.6V, Vcb=2V	1.2KΩ·μm
Polysilicon sheet resistivity, ρ_p	16.7Ω·μm
Polysilicon thickness	0.288μm
FPOLY width	6μm
FPOLY cross section area, Ap	1.73μm²
FPOLY connecting resistor, Rpe	12.57Ω
Resistance from lineN to metal, Rpc	13.74Ω
Emitter stripe length, 2W	50μm

Fig. 3. Modeled dc voltage variation in FPOLY at three different biases. The emitter stripe length is 50 μm and the width of FPOLY is 6 μm with an average sheet resistance of 58 Ω/□. The voltage is assumed to be symmetric around the center of FPOLY.

in FPOLY is given by

$$V_F(y) = C_6 - C_7 \cdot \cosh(C_4 \cdot (y - W)) \qquad (13)$$

where $C_7 = C_5 \cdot \rho_p/C_4$ and $C_6 = V_F(0) + C_7 \cosh(C_4 \cdot W)$. If the 2-D nonuniform current flow at the short edge of the emitter stripe is neglected, and we assume all the current in FPOLY flows through the resistance Rpe at the edge of base polysilicon, the edge voltage $V_F(0)$ of FPOLY and V_N are related by

$$V_F(0) = V_N - (Ap \cdot Rpe) \cdot Jp_F(0) \qquad (14)$$

and the FPOLY boundary current is given by

$$Jp_F(0) = \frac{W}{Ap(C_8 - C_1 W Rpe)} \cdot (C_3 - C_1 V_N) \qquad (15)$$

which is only a function of V_N where

$$C_8 = 1 + \frac{C_1 \rho_p}{Ap C_4^2} - \frac{C_1 \rho_p W}{Ap C_4} \coth(C_4 W). \qquad (16)$$

Once $Jp_F(0)$ is obtained, the voltage $V_F(y)$ and base current density $Jp_F(y)$ in FPOLY can be solved, which in turn gives the voltage and current distribution in the whole area of the intrinsic base region.
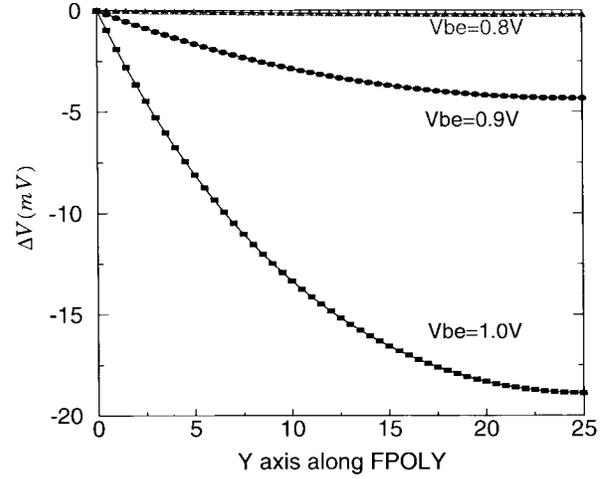
III. RESULTS AND DISCUSSION

A single metal base contact (SMB) npn BJT with an emitter stripe length of 50 μm is used for this study. The layout and cross section of the intrinsic device structures are illustrated in Figs. 1 and 2, respectively. The 2-D doping profile was determined using the process simulator Athena, and the polysilicon sheet resistance was obtained from independent measurements. The other resistances and boundary condition $J_b(0)$ required for the model are determined from 2-D device simulations using FLOODS [15], [16]. Due to the Early effect and base conductivity modulation, the base width W_b and intrinsic base resistivity ρ_b vary depending on the current injection level and need to be extracted from simulations at each bias. The required parameters for the model of the transistor are summarized in Table I.

The modeled ohmic voltage drop along FPOLY at three different biases is shown in Fig. 3. At $V_{be} = 0.8$ V, the model shows a small debiasing effect along the FPOLY and the voltage variation is less than 0.3 mV. When $V_{be} = 1$ V, the ohmic voltage drop in FPOLY is larger than 18 mV due to the larger current flow in FPOLY. However, even at this condition, $\Delta V \ll 2V_{TH} \approx 52$ mV, the linear approximation

$$C_1 = -\frac{\dfrac{Z}{\rho_b \cdot \sin(ZL)}}{1 + 2R_{bext} \cdot \left(\dfrac{Z}{\rho_b \cdot \sin(ZL)}\right)} \qquad (7)$$

$$C_2 = \frac{R_{bext} J_{bt} \cdot \left(\dfrac{Z}{\rho_b \cdot \sin(ZL)}\right) + \dfrac{2V_{TH} Z}{\rho_b} \cdot \tan\left(\dfrac{ZL}{2}\right) + \dfrac{Z}{\rho_b \cdot \sin(ZL)} \cdot V_N}{1 + 2R_{bext} \cdot \left(\dfrac{Z}{\rho_b \cdot \sin(ZL)}\right)} \qquad (8)$$

$$C_3 = \frac{R_{bext} J_{bt} \cdot \left(\dfrac{Z}{\rho_b \cdot \sin(ZL)}\right) + \dfrac{2V_{TH} Z}{\rho_b} \cdot \tan\left(\dfrac{ZL}{2}\right) - \dfrac{Z}{\rho_b \cdot \sin(ZL)} \cdot V_N}{1 + 2R_{bext} \cdot \left(\dfrac{Z}{\rho_b \cdot \sin(ZL)}\right)} \qquad (9)$$
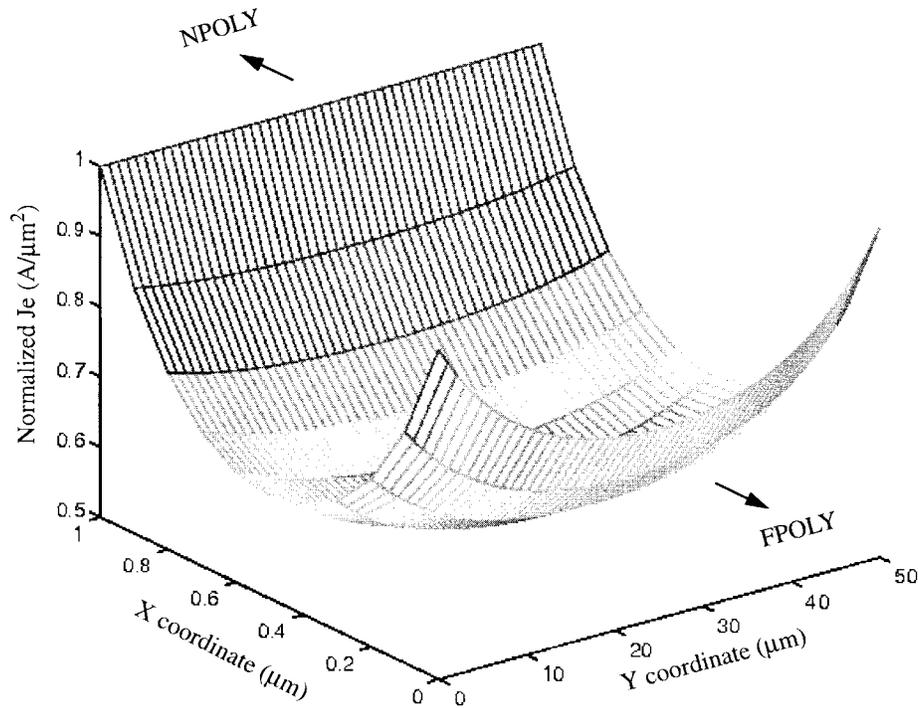
Fig. 4.   Plot of the 2-D distribution of emitter current calculated by the model. The intrinsic base sheet resistance is 4.1 $\Omega/\square$.

in deriving (5) is still valid. The emitter current density injected through the base-emitter junction may change dramatically in the presence of the debiasing effect because of its exponential dependence on the base-emitter junction voltage. Fig. 4 shows the modeled emitter current density Je beneath the emitter area when $Vbe = 1.0$ V. Je is constant along the intrinsic base edge near NPOLY because of the constant bias at NPOLY whereas Je decreases toward the center of the stripe due to the ohmic voltage drop along FPOLY in the y-direction and in the intrinsic base region along the x-direction. Thus, the emitter current crowds at the edges of the stripe. The total emitter current computed from the quasi-2-D model is smaller than that of the 2-D model [14] due to the additional debiasing effect in the y-direction.

Although the debiasing in FPOLY at low biases is very small, it still cause the voltage in FPOLY to be slightly lower than that in NPOLY. Fig. 5 compares the normalized voltage distribution along the intrinsic base region between the model and FLOODS simulations. In all cases, V_N is fixed at 0.8 V and V_F is swept from 0.8 V to 0.7994 V. Both the model and simulations show similar debiasing effects across the intrinsic base region. The discrepancy between the simulation results and the model is due to the fact that the path used to extract the potential profiles in the simulations, as indicated by the dashed line beneath the emitter in Fig. 2, does not correspond to the actual base current path assumed in the model. Note, at the minimum voltage point l of the potential profile, where $J_b(x)$ is zero, the base current injected from base to emitter on the left hand side of l is contributed by the left terminal contact (NPOLY), and the current injected on the right hand side of l comes from the right terminal contact (FPOLY). The point l acts as a current divider in the intrinsic base region. When the bias is symmetric, l is located at the center of the intrinsic
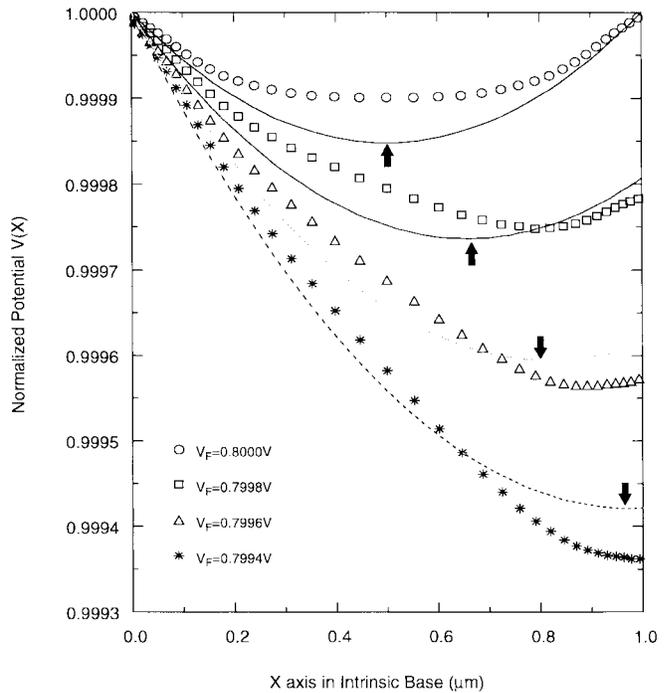

Fig. 5.   The dc potential profile in the intrinsic base region at different V_F's ($X = 1.0$ μm). In all cases, V_N ($X = 0$ μm) is fixed at 0.8 V. The symbols indicate the device simulation data and lines are the modeling results. The arrow signs indicate the positions of l points computed by the model.

base, and the current is equally divided between NPOLY and FPOLY. As V_F decreases, l moves toward FPOLY and forces part of the current originally flowing through FPOLY at symmetric bias to flow through NPOLY. Consequently, the current J_{bN} from NPOLY increases corresponding to the decrease of current J_{bN} through FPOLY.
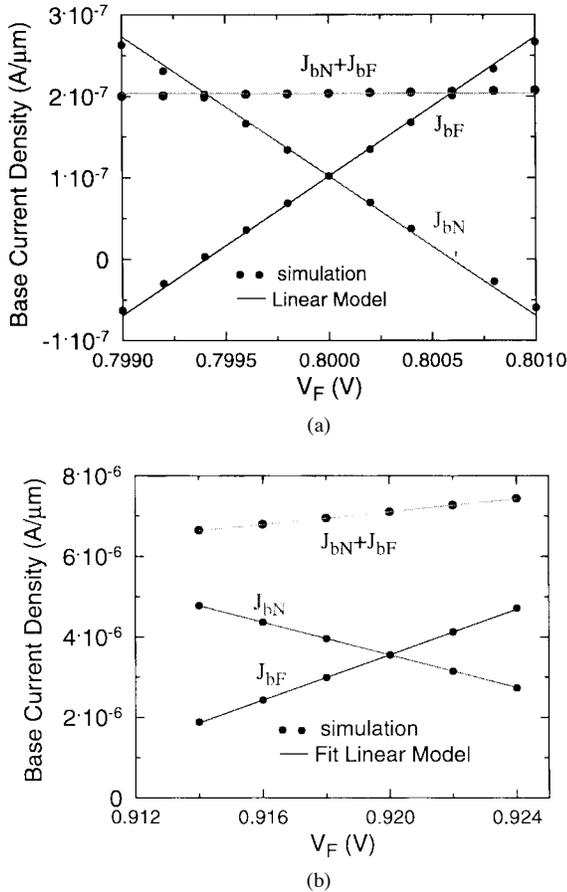
Fig. 6. Simulated and modeled polysilicon base terminal current as a function of V_F at (a) $V_N = 0.8$ V, and (b) $V_N = 0.92$ V. In (b), C_1's in (6) are adjusted to meet the decreasing total current of the simulation results.
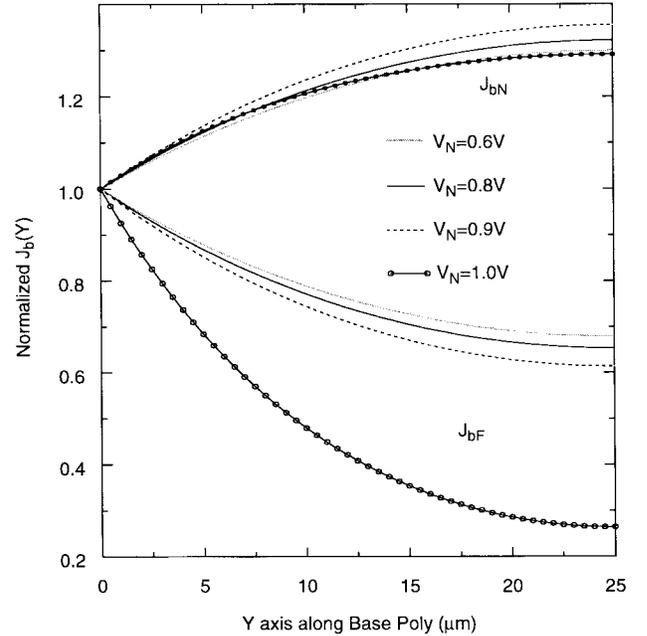

Fig. 7. Modeled dc base terminal current density injected into active base region versus position along base polysilicon at different biases. The stripe length is 50 μm and voltage in NPOLY is assumed to be uniform. The current densities J_{bN} and J_{bF} are normalized to that at $y = 0.0$ μm.

The leverage behaviors of terminal currents at asymmetric biases can be observed from Fig. 6. The FPOLY current J_{bF} decreases and NPOLY current J_{bN} increases if V_F is smaller than V_N. In the case of $V_N = 0.8$ V, the base current injected from base to emitter is approximately constant everywhere in the intrinsic base region since the voltage variation in FPOLY (refer to Fig. 3) and in the intrinsic base region is small. Thus, the reduction of J_{bF} is compensated by the increase of J_{bN}, and the total current density is approximately constant at different V_F's as shown in Fig. 6(a). As the bias increases, a more significant ohmic voltage drop takes place along FPOLY (see also Fig. 3) which reduces V_F and the voltage across the base-emitter junction, and decreases the total base current density. Fig. 6(b) shows the J-V_F relation while V_N is biased at 0.92 V. The total current reduces by 6.7% when V_F is 6 mV lower than V_N. Under these high injection conditions, the coefficient C_1 in (6a) is slightly different from C_1 in (6b). For better accuracy in the quasi-2-D model, C_1 in (6a) and (6b) is corrected according to the simulated slopes of J_{bN} and J_{bF} at high biases as illustrated in Fig. 6. Although it requires a correction in the coefficients, the linear relation between the terminal currents and V_F, i.e., (6), is valid until the voltage difference approaches $2V_{TH}$ which is at a bias exceeding the range of interest.

The modeled terminal base current densities injected from the polysilicon to the active base region along the y-direction

are shown in Fig. 7. The current, J_{bN}, injected from NPOLY is always larger than the current, J_{bF}, from FPOLY since the bias at NPOLY is higher than the bias at FPOLY. The difference between J_{bN} and J_{bF} is larger at the center than at the edge of the stripe due to the debiasing along FPOLY. Note that the decreasing current in FPOLY is compensated by the increasing current in NPOLY if V_N is less than 0.9 V. The total current is about the same as that without considering the debiasing effect in FPOLY. However, when V_N is larger than 0.9 V, the current decrease in FPOLY is larger than the increase in NPOLY because of the significant ohmic voltage drop in FPOLY. The total current is less than that without taking into account the debiasing effect in FPOLY.

IV. BASE RESISTANCE

For a symmetric double polysilicon, double metal base contact structure, the base current contributed from each side of the polysilicon base should be the same. However, for the single metal base contact device as illustrated in Fig. 1, the current contributed by FPOLY is less than that from NPOLY due to the asymmetric bias as has been discussed above. Fig. 8 shows the ratio of base current contributed from FPOLY and NPOLY as a function of bias. Note that even at low biases, the ratio is less than 40% and falls off slightly as the bias increases. For biases larger than 0.9 V, the ratio decreases very fast due to the significant debiasing effect in FPOLY.

The current flowing through FPOLY experiences a larger base resistance than that through NPOLY. Since the current via FPOLY decreases and the current associated with NPOLY increases at higher biases, it implies more and more current flows through the low resistive path as the bias increases. Thus, both the current crowding effect in the intrinsic base
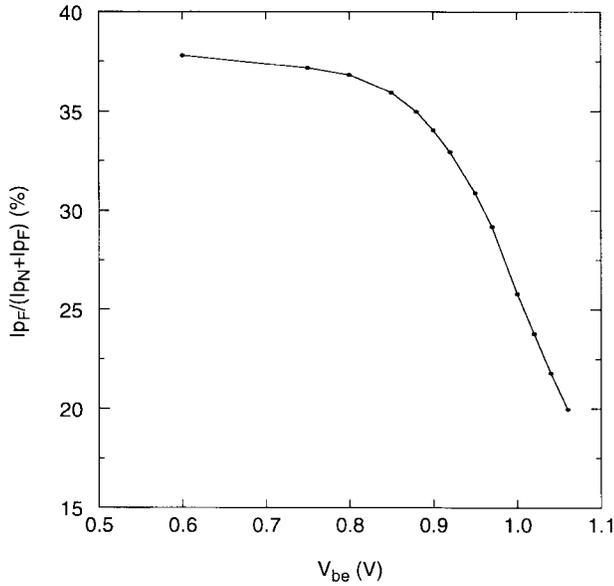
Fig. 8. The ratio of base current contributed by FPOLY, $I_{\rm PF}$, to the total current, $I_{\rm PF} + I_{\rm PN}$, as a function of bias calculated by the quasi-2-D model, where IPN is the current contributed by NPOLY.
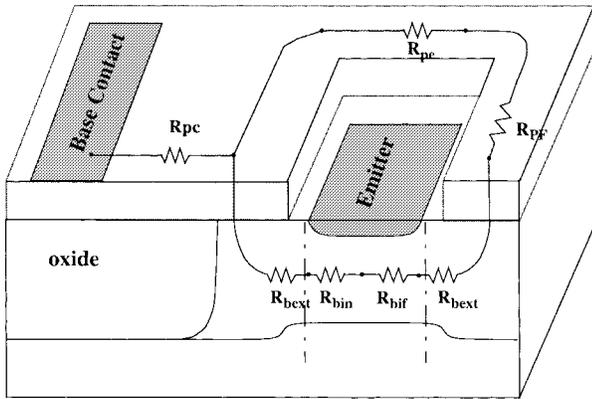

Fig. 9. The diagram of the long stripe BJT structure and the definition of the base resistance in each subregion. The lightly shaded area is the base polysilicon region. Rpc, Rpe, and R_{bext} are the constant lumped resistances. $R_{\rm bin}$, $R_{\rm bif}$, and $R_{\rm PF}$ are functions of the base current.

region and the current re-distribution in the polysilicon base region contribute to the decrease of base resistance as the bias increases.

The total base resistance R_b can be calculated using the dissipated power method [17]

$$P_b = I_b^2 R_b = \sum_i \int_{v_i} J_b \cdot \nabla V_b \cdot dv_i \qquad (17)$$

where v_i is the volume of the region interested, I_b is the total base current, J_b is the current density flowing through v_i, and is the gradient of potential in the direction of current flow. Fig. 9 shows the division of regions used in quasi-2-D model to compute the individual power dissipation in each region. The total power dissipation P_b is

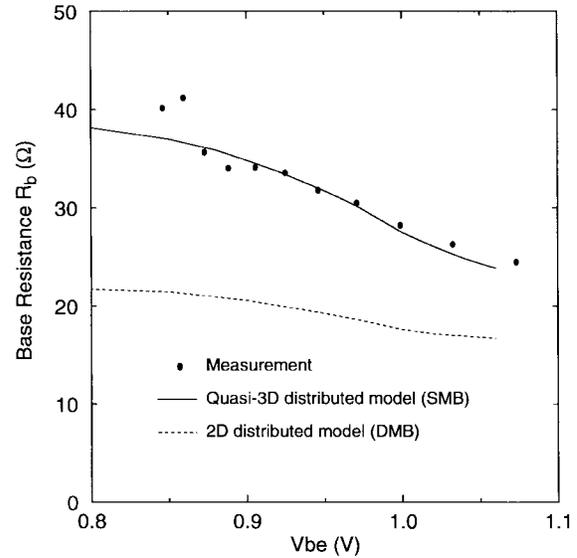$$P_{\rm BIF} + P_{\rm BIN} + P_{\rm PF} + P_{\rm BEN} + P_{\rm BEF} + P_{\rm PC} + P_{\rm pe} \qquad (18)$$

Fig. 10. A comparison of dc base resistances obtained from measurements, 2-D, and quasi-2-D base distributed models. The emitter stripe length is 50 μm and the width of the FPOLY in the device is 6 μm.

where $P_{\rm PC} = I_b^2 R_{\rm PC}$ is the power dissipated in NPOLY through a lumped resistance $R_{\rm PC}$. $P_{\rm pe} = 2R_{\rm pe} \cdot (ApJp_F(0))^2$ is the power loss in the polysilicon connection between NPOLY and FPOLY. $P_{\rm BEN}$ and $P_{\rm BEF}$ are dissipated power in the extrinsic base regions due to lumped resistances, R_{bext}, connected to NPOLY and FPOLY, respectively. $P_{\rm PF}$ is the power consumption in FPOLY, $P_{\rm BIF}$ and $P_{\rm BIN}$ are the power loss in the intrinsic base regions due to the current flow associated with FPOLY and NPOLY, respectively. Since the base current and voltage in each region have been obtained from the quasi-2-D model, the total dissipated power and base resistance can be solved easily.

A 2-D distributed model or a 2-D device simulation can be used to compute the base resistance of a symmetric double metal base contact device structure (DMB) [17]. However, these methods cannot be used to calculate the base resistance of a SMB structure since the current path modulation in the intrinsic base region and current re-distribution in the polysilicon region are not included. For the same transistor, using a 2-D model describing a DMB layout to predict the base resistance of a SMB layout is expected to have a significant error. Fig. 10 compares the base resistances of a SMB transistor computed by the 2-D and quasi-2-D models with those obtained from measurement. The Gummel-plot method [18] is used to measure the dc base resistance. The base resistance of the quasi-2-D model is seen to be much larger and more accurate than that of the 2-D model in the bias range of interest. The analysis of the power dissipation in each region shows the major difference comes from three facts: 1) the current flowing through NPOLY in the quasi-2-D model has longer current paths in the intrinsic base region and thus higher effective resistance than that of the 2-D model due to the movement of the minimum voltage point toward FPOLY; 2) the highly resistive current path of FPOLY in the quasi-2-D model; and 3) $R_{\rm PC}$ in the 2-D model is one half of $R_{\rm PC}$ in the quasi-2-D model due to the additional metal
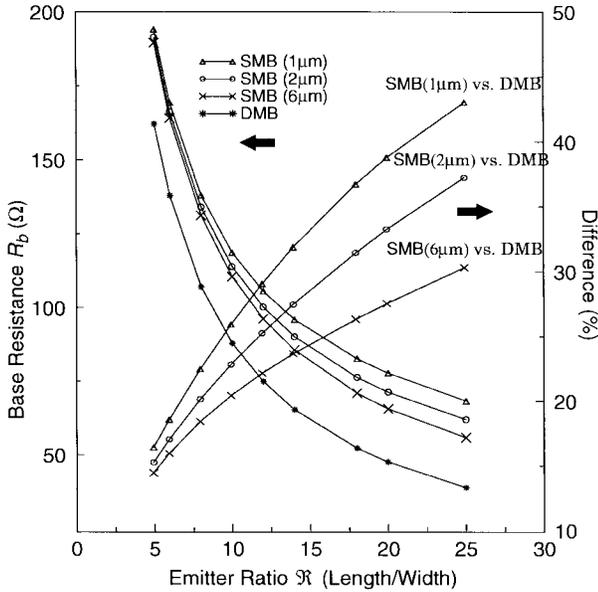
Fig. 11. The plot of the modeled base resistance and difference between SMB and DMB structures as a function of emitter stripe ratio with different FPOLY widths. The sheet resistance of FPOLY is 58 $\Omega/\square$ and FPOLY width is indicated in the parenthesis.
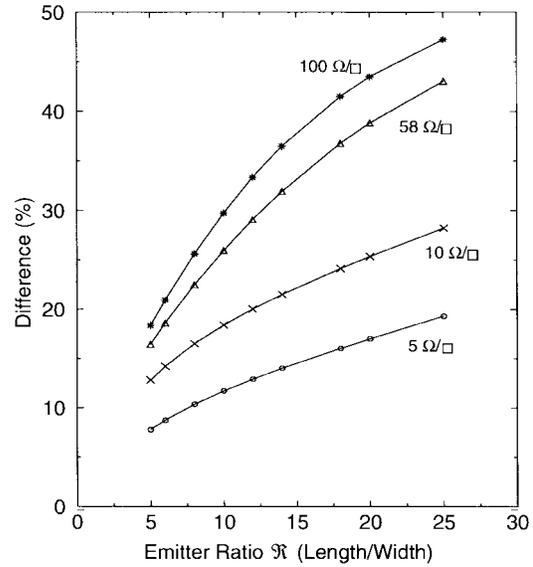

Fig. 12. The difference of base resistance between SMB and DMB structures as a function of emitter stripe ratio with different FPOLY sheet resistances. The width of FPOLY is 1 μm and $V_{be} = 0.9$ V.

base contact in DMB structure. As the bias increases, the base resistance of the 2-D model mainly decreases due to current crowding and conductivity modulation in the intrinsic base region. In addition to the these mechanisms, the current re-distribution from high to low resistive paths in the polysilicon region further reduces the base resistance in the quasi-2-D model as the bias increases. The variation of base resistance computed by the quasi-2-D model is thus larger and more accurate than that of the 2-D model as can be seen in Fig. 10.

Fig. 11 shows the modeled base resistance plotted as a function of emitter stripe ratio $\Re$ with three different FPOLY widths, λ, while V_{be} is biased at 0.9 V. As expected, the base resistance of DMB decreases inversely proportional to the increase of stripe length. The R_b of SMB always has higher values than that of DMB and the device with a narrower λ results in a larger R_b. The difference of R_b between these two structures is also included in Fig. 11. It is shown that the difference is small for the shorter stripe device and becomes larger as the stripe length increases because the distributed effects are more significant at a longer FPOLY. Scaling of the FPOLY width further enlarges the difference. For example, $\Re$ if is 10, R_b of SMB with $\lambda = 1$ μm is 26% higher whereas R_b of SMB with $\lambda = 2$ μm is 23% higher than R_b of DMB.

Silicided polysilicon technologies are often utilized in contemporary high-speed double polysilicon BJT's to reduce the base resistance. However, this process increases the complexity of process and cost. Fig. 12 shows the difference of R_b between DMB and SMB structures computed with different polysilicon sheet resistances and $\Re$. For a nonsilicided polysilicon with a sheet resistance of 100 $\Omega/\square$, R_b of SMB with $\Re = 6$ is 21% higher than R_b of DMB. The difference increases to 36% if $\Re = 14$. If the sheet resistance is reduced to 5 $\Omega/\square$, the difference decreases but is still significant for large $\Re$. Therefore, the design of SMB structure using

symmetric device simulations without taking into account the distributed effects can significantly underestimate the base resistance. The results also suggest the R_b of DMB device is always much smaller than SMB structure unless a low sheet resistance polysilicon is used. The silicided technology is thus very important for the performance of SMB structure.

V. CONCLUSION

A quasi-2-D model describing the distributed base voltage and current in both the intrinsic and polysilicon base regions has been derived. The results illustrate the nonuniform characteristics of voltage and current in a long stripe transistor that cannot be properly described by a 2-D model. A current re-distribution effect in the polysilicon base regions due to the asymmetric bias modulation has been presented. In addition to the current crowding effect in the intrinsic base, this current re-distribution effect also plays a key role in determining the bias dependent base resistance. The base resistance has been computed from the solution of the model and the accuracy has been verified by the measured data. The same concept and methodology can be applied to analyze the distributed effects in the long interdigitated structures.

REFERENCES

[1] D. D. Tang and P. M. Solomon, "Bipolar transistor design for optimized power-delay logic circuits," *IEEE J. Solid-State Circuits*, vol. SC-14, pp. 679–684, Aug. 1979.

[2] P. Spiegel, "Transistor base resistance and its effect on high-speed switching," *Solid-State Design*, pp. 15–18, Dec. 1965.

[3] S. P. Gaur, "Performance limitations of silicon bipolar transistors," *IEEE J. Solid-State Circuits*, vol. SC-14, pp. 337–343, Apr. 1979.

[4] A. van der Ziel, "Noise in junction transistors," *Proc. IRE*, pp. 1019–1038, June 1958.

[5] K. Aufinger et al., "Noise characteristics of transistors fabricated in an advanced silicon bipolar technology," *IEEE Trans. Electron Devices*, vol. 43, pp. 1533–1538, 1996.

[6] J. S. Yuan et al., "A physics-based current-dependent base resistance model for advanced bipolar transistors," *IEEE Trans. Electron Devices*, vol. 35, pp. 1055–1062, 1988.

[7] H. Satake and T. Hamasaki, "Low-temperature (77K) BJT model with temperature dependences on the injected condition and base resistance," *IEEE Trans. Electron Devices*, vol. 37, pp. 1688–1697, 1990.

[8] T. Fuse et al., "A physically based base pushout model for submicrometer BJT's in the presence of velocity overshoot," *IEEE Trans. Electron Devices*, vol. 39, pp. 396–403, 1992.

[9] H. S. Rhee, S. Lee, and B. R. Kim, "DC and A.C. current crowding effects model analysis in bipolar junction transistors using a new extraction method," *Solid-State Electron.*, vol. 38, no. 1, pp. 31–35, 1995.

[10] H. N. Ghosh, "A distributed model of the junction transistor and its application in the prediction of the emitter-base diode characteristics, base impedance, and pulse response of the device," *IEEE Trans. Electron Devices*, vol. ED-12, pp. 513–531, 1965.

[11] M. P. J. G. Versleijen, "Distributed high-frequency effects in bipolar transistors," in *IEEE Bipolar Circuits Technol. Meet.*, 1991, pp. 85–88.

[12] H. Cho and D. E. Burk, "A simple model for distributed base impedance with AC verification using S-parameters measurements," in *IEEE Bipolar Circuits Technol. Meet.*, 1990, pp. 106–109.

[13] M. Schroter, "Simulation and modeling of the low-frequency base resistance of bipolar transistors and its dependence on current and geometry," *IEEE Trans. Electron Devices*, vol. 38, pp. 538–544, 1991.

[14] J. R. Hauser, "The effects of distributed base potential on emitter-current injection density and effective base resistance for stripe transistor geometries," *IEEE Trans. Electron Devices*, vol. ED-11, pp. 238–242, 1964.

[15] M. Liang and M. E. Law, "An object-oriented approach to device simulation-FLOODS," *IEEE Trans. Computer-Aided Design*, vol. 13, pp. 1235–1240, Oct. 1994.

[16] ———, "Influence of lattice self-heating and hot-carrier transport on device performance," *IEEE Trans. Electron Devices*, vol. 41, pp. 2391–2398, Dec. 1994.

[17] E. Dubois et al., "Accuracy of series resistances extraction schemes for polysilicon bipolar transistors," in *IEEE Bipolar Circuits Technol. Meet.*, 1994, pp. 148–151.

[18] T. Fuse and Y. Sasaki, "An analysis of small-signal and large signal base resistance for submicrometer BJT's," *IEEE Trans. Electron Devices*, vol. 42, pp. 534–539, Mar. 1995.

Mark E. Law (S'79–M'81–SM-92) received the Ph.D. degree from Stanford University, Stanford, CA, in 1988.

Upon graduation, he spent one year at Stanford University as a Research Associate. During this time, he coauthored the SUPREM–IV process simulator and his research focused on the modeling of point defects and dopant diffusion in silicon. He joined the University of Florida, Gainesville, as an Assistant Professor in December 1988, and was promoted to Associate Professor in August 1993, and Professor in August 1997. He has written over 100 papers in the area of process and device modeling. He has been working in this field for over fifteen years as a professor, student and engineer for Hewlett Packard. His research interests are in integrated circuit process and has funding from SRC, Sematech, in this area.

Dr. Law was named a National Science Foundation Presidential Faculty Fellow in 1992, and earlier he had won an IBM Young Investigator Award. SRC recognized his research by awarding his research group the Technical Excellence Award. Iowa State University named him an Outstanding Young Alumnus for 1994. He won a 1995 Teaching Improvement Program Award from the University of Florida, and won the 1996–1997 College of Engineering Teacher of the Year Award. He has served on the technical committees of the Bipolar Circuits and Technology Meeting (BCTM), the International Electron Device Meeting (IEDM), the Numerical Process and Device Simulation Workshop (NUPAD), and the Simulation of Semiconductor Processes and Devices conference. He served as guest editor for a special issue of the IEEE TRANSACTIONS ON COMPUTER-AIDED DESIGN devoted to the proceedings of NUPAD, served as an Associate Editor for IEEE TRANSACTIONS ON SEMICONDUCTOR MANUFACTURING from 1994 to 1997, served as the technical program committee chairman for the 1994 NUPAD, and is the 1997 chairman of the SISPAD conference. He is currently the editor of IEEE JOURNAL ON SEMICONDUCTOR TECHNOLOGY COMPUTER-AIDED DESIGN. He has also worked on the 1994 and 1997 Semiconductor Industrial Association roadmap for semiconductor technology. He is a member of the Electrochemical Society, the American Physical Society, the American Society for Engineering Education, the American Association for the Advancement of Science, Phi Kappa Phi, Tau Beta Pi, Eta Kappa Nu, and Sigma Xi.

Kenneth O (S'86–M'89) was born in Seoul, Korea, in 1960. He received the S.B., S.M., and Ph.D. degrees in electrical engineering and computer science from the Massachussetts Institute of Technology, Cambridge, in 1984, 1984, and 1989, respectively. For his Ph.D. dissertation, he developed a BiCMOS process utilizing selective epitaxial growth for analog-digital applications. Using the process, he has also demonstrated a merged BiMOS transistor concept.

Between 1984 and 1985, he worked as a Process Engineer at Harris Corporation, Melbourne, FL. From 1989 to 1994, he worked at Analog Devices Inc., developing submicrometer CMOS processes for mixed-signal applications, as well as examining issues for Si-Ge HBT technologies for analog applications. In 1994, he joined the faculty of the Department of Electrical and Computer Engineering, University of Florida, Gainesville, as an Assistant Professor. He teaches digital, analog, and microwave circuits courses at both the undergraduate and graduate levels. This year, he has created and taught a course entitled "RF Integrated Circuits and Technologies for Wireless Applications." His research group [Silicon Microwave Integrated Circuits and Systems Research Group (SiMICS)] is developing circuits and passive components required to implement analog and digital systems operating between 1 and 20 GHz using silicon IC technologies.

Dr. O served as a Member of the Technical Program Committee for the IEEE Bipolar/BiCMOS Circuits and Technology Meeting between 1992 and 1994. In 1995 and 1996, he served as the Short Course Chairman for the same conference. He has authored and coauthored approximately 25 journal and conference publications, as well as holding four patents. He has received the 1995 and 1997 IBM Faculty Development Awards and the 1996 NSF Early Career Development Award.

Ming-Yeh Chuang was born in Taiwan, R.O.C., in 1964. He received the B.S. degree from Tamkang University, Taiwan, in 1986, and the M.S. degree from the University of Florida, Gainesville, in 1993, both in electrical engineering. Since 1993, he has been pursuing the Ph.D. degree in electrical engineering at the University of Florida. His research interests are in simulating and modeling physical processes in semiconductor devices, specifically high-frequency transistors. His work involves the development of the general purpose device simulator FLOODS for analysis of advanced semiconductor devices.